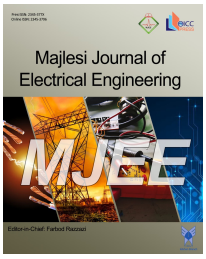

Volume 19, Issue 2, 192540 (1-7)

Majlesi Journal of Electrical Engineering (MJEE)

https://doi.org/10.57647/j.mjee.2025.1902.40

Performance evaluation of CA-, GO- and SO-CFAR processors in a non-centered Lévy-distributed clutter

El-Hadi Meftah[1,*], Abdelhalim Rabehi[2], Slimane Benmahmoud[3]

[1]*LISIC Laboratory, Faculty of Electrical Engineering, USTHB, Bab-Ezzouar, Algiers, Algeria.*
[2]*Laboratory of Telecommunications and Smart Systems, University of Ziane Achour, Djelfa, Algeria.*
[3]*Department of Electronic Engineering, University of M'sila, M'sila, Algeria.*

[*]**Corresponding author:** elhadi.meftah@usthb.edu.dz

Original Research

Received:
30 November 2024
Revised:
19 March 2025
Accepted:
13 April 2025
Published online:
1 June 2025

Abstract:

Constant false alarm rate (CFAR) processors are critical for radar reliable target detection in radar systems. Traditional CFAR designs often assume Gaussian clutter, which may not reflect real-world conditions. Lévy distributions, with heavy tails and a location parameter (δ), provide a more accurate model for non-Gaussian and non-centered clutter in complex environments. This paper presents a comprehensive performance analysis of three widely used CFAR processors-cell-averaging (CA), greatest-of (GO), and smallest-of (SO) in homogeneous Lévy-distributed clutter with an arbitrary δ. We derive integral-form expressions for the probability of false alarm (PFA) for each processor, explicitly incorporating δ. Furthermore, we provide analytical formulations for the probability density function (PDF) of key statistics involving Lévy random variables, such as sums, minima, and maxima. Monte Carlo simulations validate the theoretical results, showing that the PFA performance improves with increasing δ, highlighting the critical impact of clutter location on CFAR detector performance. These findings offer valuable insights for designing robust CFAR detectors in non-Gaussian, non-centered clutter environments.

Keywords: Cell-averaging constant false alarm rate; Constant false alarm rate processors; Greatest-of constant false alarm rate; Lévy-distributed clutter; Probability of false alarm; Smallest-of constant false alarm rate

1. Introduction

In radar target detection, clutter refers to unwanted reflections from objects that can interfere with the detection of real targets. Under these conditions, Constant False Alarm Rate (CFAR) techniques are applied to maintain a fixed false alarm rate in homogeneous clutter environments. CFAR processors adaptively set detection thresholds by estimating the clutter level from reference cells surrounding the cell under investigation (CUI). Several CFAR variants have been developed to address different clutter scenarios [1–4]. Traditional Cell-Averaging CFAR (CA-CFAR) detectors estimate clutter level using the mean of surrounding cells [5], but their performance degrades in non-homogeneous clutter. To address these limitations, the Greatest Of CFAR (GO-CFAR), initially proposed by Hansen and Sawyers [6], employs the maximum of the sums from the leading and lagging reference windows for clutter level estimation, improving robustness in clutter transition regions. Weiss in [7] further analyzed GO-CFAR's performance in multi-target scenarios. In parallel, the SO-CFAR (Smallest Of CFAR) method, developed by Trunk [8] in the context of target resolution, mitigated the effects of target masking. Rickard and Dillard in [9] provided an early, comprehensive analysis of adaptive detectors, including SO-CFAR, laying the theoretical and practical foundations for their use in diverse environments. These foundational works paved the way for advanced applications of GO-CFAR and SO-CFAR in modern radar systems [10–14].

Modern high-resolution radars face challenges in statistical clutter modeling due to increased complexity. The radar's research community has proposed various non-Gaussian models to better represent high-resolution radar clutter, including Positive Alpha-Stable, Weibull, Log-Normal, Pareto, and K-distributions [15–19]. However, adopting these non-Gaussian models in CFAR schemes can make deriving closed-form expressions for key performance metrics, such as probability of detection and false alarm rate, challenging or even impossible. This complicates the evaluation and optimization of CFAR detectors in complex clutter environments.

To address these challenges, advanced techniques are actively developed. These include adaptive clutter modeling methods, which dynamically select the most appropriate clutter distribution based on observed data, and robust CFAR algorithms designed to maintain detection performance across a wide range of clutter distributions [20]. Further studies have explored CFAR performance in various clutter distributions. Tsakalides et al. [21] evaluated CFAR processors in Pearson-distributed clutter, while Meziani and Soltani [22] analyzed CFAR detectors in both homogeneous and non-homogeneous Pearson-distributed environments. These works highlight the importance of understanding CFAR behavior across different non-Gaussian clutter models. Given the specific challenges posed by sea clutter, significant research has focused on target detection in such environments. Specifically, recent work has explored persymmetric adaptive target detection with dual-polarization in compound Gaussian sea clutter with inverse Gamma texture [23], and adaptive persymmetric subspace detection in non-Gaussian sea clutter with structured interference [24]. More recently, developments in this field have included machine learning (ML)-based approaches, benefiting from neural networks (NN) as well as other artificial intelligence (AI) techniques, with the aim of improving target detection in non-Gaussian and heterogeneous clutter environments [25].

In addition, numerical approximation methods have been developed to estimate some performance parameters when analytical solutions are not readily available or are difficult to predict. These methods have been deployed with the aim of optimizing radar detection performance in increasingly complex and diverse interference environments, which are characteristic of modern radar systems [26]. Indeed, the integration of theoretical insights with practical applications has led to significant progress in improving the reliability and efficiency of radar systems in challenging real-world scenarios. In particular, considerable progress has been made in the analysis of CFAR processors operating in various clutter environments. Within Weibull-distributed clutter environments, the performance of SO-CA CFAR detectors has been investigated for their ability to maintain a stable false alarm probability (PFA). In this regard, the authors in [27] evaluated these detectors by deriving analytical expressions for P_{FA} in homogeneous and non-homogeneous conditions. Their results showed that SOCA-CFAR detectors provide enhanced robustness in severe clutter environments while maintaining a low P_{FA}. Moreover, the authors of [28] have proposed a theoretical framework for the evaluation of CFAR detectors under realistic conditions, based on generalized expressions for the P_{FA} of CFAR detectors in heterogeneous environments. These expressions take into account complex clutter distributions, such as Gamma and Weibull, and enable a comparative analysis of the performance of CA-, GO- and OS-CFAR detectors. In turn, Garvanov [29] investigated the probability characteristics of CFAR processors in the presence of randomly arriving impulse interference. The author modeled this interference as binomial pulse sequences and derived analytical expressions for the P_{FA} of CA-CFAR and binary integration detectors (BI-CFAR). The results demonstrated the adaptability of these detectors for efficient operation in noisy environments, while maintaining a stable P_{FA}.

In the context of specific radar architectures, the authors of [30] analyzed the performance of CFAR detectors in multiple-input multiple-output (MIMO) radars operating in distributed gamma clutter. Specifically, they derived closed-form PFA expressions for CA-, GO- and SO-CFAR detectors and validated these expressions using Monte Carlo simulations. The results revealed that CA-CFAR detectors perform best for a small number of nodes, while GO- and SO-CFAR detectors are more efficient as the number of nodes increases. To address nonhomogeneous clutter challenges, Zhou et al. [31] proposed a robust CFAR detector using weighted amplitude iteration for more accurate detection threshold estimation, demonstrating improved performance in complex maritime environments. Subsequently, the same authors [32] developed a maximum likelihood detector for Gamma-distributed sea clutter, leveraging the statistical properties of the distribution to achieve optimized detection performance with high detection probabilities and a low false alarm rate. These findings emphasize the importance of tailoring CFAR techniques to specific clutter distributions. Finally, Sahed et al. in [33] recently derived exact analytical P_{FA} expressions for CA- and GO-CFAR detectors in Gamma-distributed clutter, which exhibit excellent agreement with Monte Carlo results.

Building upon previous findings, this paper investigates the largely unexplored performance of CFAR processors in non-centered Lévy-distributed clutter. The motivation stems from two critical observations: (i) heavy-tailed distributions like the Lévy distribution have demonstrated superior accuracy in modeling modern radar clutter phenomena, especially in high-resolution maritime environments; and (ii) conventional Gaussian-based models essentially fall short of capturing the asymmetric and impulsive nature of these situations. To bridge this gap, we derive closed-form expressions for the P_{FA} of CA-, GO-, and SO-CFAR processors operating in homogeneous non-centered Lévy-distributed clutter.

The main contributions of this paper are summarized as follows:

- We have derived accurate formulations for the PDF of the sum, the minimum of two sums, and the maximum of two sums of independent and identically distributed (i.i.d) non-centered Lévy random variables (RVs). These formulations provide a solid mathematical foundation for analyzing CFAR processors in non-Gaussian clutter environments.
- We have derived novel integral-form expressions for the P_{FA} CA-, GO-, and SO-CFAR processors, assuming an arbitrary location parameter δ. These expressions generalize existing CFAR analyses, which often rely on simplified clutter models (e.g., Gaussian or centered distributions), providing a more realistic and adaptable framework.
- We have rigorously validated the theoretical results through both numerical evaluations of the analytical ex-

pressions and extensive Monte Carlo simulations. The consistency between these independent approaches confirms the accuracy and reliability of the derived formulations.

- This work provides a detailed performance evaluation of CA-, GO-, and SO-CFAR processors in homogeneous non-centered Lévy-distributed clutter environments. By analyzing how the location parameter influences the P_{FA}, we offer valuable insights into the behavior of these processors in complex radar scenarios. The results highlight the sensitivity of CFAR performance to clutter characteristics, emphasizing the need for robust detection strategies in non-Gaussian environments.

The Remainder of this paper is organized as follows: Section 2 describes the three CFAR processors considered in this work and states the associated assumptions. Section 3 introduces novel and important statistical findings related to the clutter's mean level. These findings are utilized in section 4, which provides an analytical evaluation of the processors' PFAs. Section 5 presents extensive numerical results, including simulations and comparative analyses, to validate the theoretical findings and demonstrate the practical implications of the proposed approaches. Finally, section 6 summarizes the key contributions of the work, discusses potential limitations, and outlines directions for future research.

This paper employs the following standard notations $f_X(x)$, $F_X(x)$, and $\mathbb{E}[X]$ or μ_X denote, respectively, the probability density function (PDF), the cumulative distribution function (CDF), and the expectation of the random variable (RV)X. "erf" $(\cdot)$ is the error function (also called the Gauss error function) [34, equation (8.250.1)], and "erfc" $(\cdot)$ is the complementary error function [34, equation (8.250.4)].

2. CFAR processors' description and related assumptions

All In CFAR processors, the output statistic Z, which estimates the clutter level, is computed by processing the contents of $2N$ reference cells surrounding the cell under test (CIT), denoted as X_0. For the three CFAR processors considered in this work the statistic Z is defined as follows:

$$Z = \begin{cases} \frac{1}{2N}(Z_1+Z_2), & \text{if CA-CFAR,} \\ \frac{1}{N}\max(Z_1+Z_2), & \text{if GO-CFAR,} \\ \frac{1}{N}\min(Z_1+Z_2), & \text{if SO-CFAR,} \end{cases} \tag{1}$$

where $Z_1 = \sum_{i=1}^{N} X_i$ and $Z_2 = \sum_{i=N+1}^{2N} X_i$ denote the sums of the leading and lagging reference windows, respectively. X_i, $i \in \{1,2,\ldots,2N\}$ denote the contents of the reference cells surrounding the cell under investigation (CUI) whose content is X_0. N denotes the size of the reference window.

To determine whether a target is present (hypothesis H_1) or absent hypothesis H_2 in the CUI, a binary hypothesis test is performed as follows:

$$X_0 \underset{H_0}{\overset{H_1}{\gtrless}} TZ \tag{2}$$

where T in (2) is the scaling factor used to achieve the desired P_{FA} for a given window of size $2N$ when the total clutter is homogeneous. The scaling factor ensures that the detection threshold adapts to the clutter level estimated from the reference cells.

To analyze the P_{FA} of different considered CFAR processors in the presence of a homogeneous clutter, we make the following assumptions. First, the square-law detected outputs X_i is a Lévy RV whose PDF and CDF are given in Definition 1 in section 3. Second, statistical independence is assumed among all observations within the $2N+1$ cells, which include the CUI, exhibit statistical independence. These assumptions provide the basis for deriving analytical expressions for P_{FA} and conducting a rigorous mathematical analysis of CFAR performance in the presence of non-centered Lévy clutter, offering insights into realistic non-Gaussian environments.

3. Statistical preliminaries and key results

In this section, we review key statistical preliminaries from the theory of RVs, focusing on properties relevant to CFAR processor analysis. These preliminaries form the basis for modeling clutter using non-centered Lévy-distributed RVs. We then present significant findings on the statistical behavior of sums, minimums, and maximums of i.i.d. Lévy RVs. These results are crucial for characterizing clutter level estimates and will be applied in section 4 to evaluate the P_{FA} for the CA-, GO-, and SO-CFAR processors.

3.1 Statistical preliminaries

Definition 1. A RV X following a non-centered Lévy distribution with location parameter δ and a scale parameter γ is denoted by Lévy (δ,γ). Its PDF and CDF using the location-scale parametrization are given, respectively, by

$$f_X(x) = \sqrt{\frac{\gamma}{2\pi}}\frac{e^{-\frac{\gamma}{2(x-\delta)}}}{(x-\delta)^{\frac{3}{2}}} \quad \text{for } x \geq \delta, \gamma > 0 \tag{3}$$

$$F_X(x) = \operatorname{erfc}\left(\sqrt{\frac{\gamma}{2(x-\delta)}}\right) \quad \text{for } x \geq \delta, \gamma > 0 \tag{4}$$

Remark 1: Setting the location parameter $\delta = 0$ yields a centered Lévy distribution, which corresponds to a heavy-tailed Pearson distribution. This model has been shown to be effective for modeling data such as impulsive signals, active sonar returns, and marine clutter. Its ability to capture impulsive behavior makes it particularly suitable for these applications [2, 5, 14, 27].

Remark 2 In various contexts, such as signal processing or finance, clutter or data often exhibit extreme values or outliers that are better captured by heavy-tailed distributions. As a special case of the inverse Gamma distribution, the Lévy distribution is particularly suitable for modeling radar clutter due to its heavy-tailed nature. Unlike Gaussian-like distributions, it allows for the occurrence of extremely large values with higher probability, making it an ideal choice for scenarios involving impulsive or complex clutter behavior [34].

3.2 Key results

Lemma 1 Let $\{X_i\}_{i=1}^{2N}$ be a sequence of i.i.d. RVs, where $X_i \sim$ Lévy(δ,γ). The PDF and CDF of RV $Z=\sum_{i=1}^{2N} X_i$ are given, respectively, as follows:

$$f_z(z)=\sqrt{\frac{2N^2\gamma}{\pi}}\frac{e^{-\frac{2N^2\gamma}{z-2N\delta}}}{(z-2N\delta)^{\frac{3}{2}}} \quad z\geq 2N\delta,\gamma>0 \tag{5}$$

$$F_z(z)=\operatorname{erfc}\left(\sqrt{\frac{2N^2\gamma}{z-2N\delta}}\right) \quad z\geq 2N\delta,\gamma>0 \tag{6}$$

Proof: The characteristic function $\varphi_Z(w)$ of Z is defined as:

$$\varphi_Z(w)=E[e^{jwZ}]=E[e^{jw\sum_{i=1}^{2N}X_i}]=(E[e^{jwX_1}])^{2N} \tag{7}$$

$$\begin{aligned}\varphi_Z(w)=&(E[e^{jwX_1}])^{2N}=\left(\int_0^{+\infty}e^{jwX_1}f_{X_1}(x_1)dx_1\right)^{2N}\\ =&\left(\sqrt{\frac{\gamma}{2\pi}}\underbrace{\int_0^{+\infty}\frac{e^{jwx}-\frac{\gamma}{2(x-\delta)}}{(x-\delta)^{\frac{3}{2}}}}_{=I}\right)^{2N}\end{aligned} \tag{8}$$

After evaluating the integral I, equation (8) can be inverted using the Fourier transform to yield the result in (5). The CDF in (6) can be easily derived by integrating the PDF obtained in (5). This completes the proof.

Lemma 2 Let $\{X_i\}_{i=1}^{2N}$ be a sequence of i.i.d. RVs, where $X_i \sim$ Lévy(δ,γ). Define $Z_1=\sum_{i=1}^{N}X_i$ and $Z_2=\sum_{i=N+1}^{2N}X_i$. The PDF of RV $Z=\max(Z_1,Z_2)$ is given by:

$$f_z(z)=2\sqrt{\frac{N^2\gamma}{\pi}}\frac{e^{-\frac{N^2\gamma}{z-N\delta}}}{(z-N\delta)^{\frac{3}{2}}}\operatorname{erfc}\left(\sqrt{\frac{N^2\gamma}{(z-N\delta)}}\right), z\geq N\delta,\gamma>0 \tag{9}$$

Proof: The PDF of $Z=\max(Z_1,Z_2)$ can be expressed as:

$$f_z(z)=2f_{Z_i}(z)F_{Z_i}(z),\ i\in\{1,2\} \tag{10}$$

From Lemma 1, the PDF and CDF of Z_i (for $i\in\{1,2\}$) are given, respectively, as follows:

$$f_{Z_i}(z)=\sqrt{\frac{N^2\gamma}{\pi}}\frac{e^{-\frac{N^2\gamma}{z-N\delta}}}{(z-N\delta)^{\frac{3}{2}}}, z\geq N\delta,\gamma>0 \tag{11}$$

$$F_{Z_i}(z)=\operatorname{erfc}\left(\sqrt{\frac{N^2\gamma}{z-N\delta}}\right), z\geq N\delta,\gamma>0 \tag{12}$$

Substituting (11) and (12) into (14) yields the result in (9).

Lemma 3 Let $\{X_i\}_{i=1}^{2N}$ be a sequence of i.i.d. RVs, where $X_i \sim$ Lévy(δ,γ). Define $Z_1=\sum_{i=1}^{N}X_i$ and $Z_2=\sum_{i=N+1}^{2N}X_i$. The PDF of RV $Z=\min(Z_1,Z_2)$ is given by:

$$f_z(z)=2\sqrt{\frac{N^2\gamma}{\pi}}\frac{e^{-\frac{N^2\gamma}{z-N\delta}}}{(z-N\delta)^{\frac{3}{2}}}\operatorname{erfc}\left(\sqrt{\frac{N^2\gamma}{z-N\delta}}\right), z\geq N\delta,\gamma>0. \tag{13}$$

Proof: The PDF of $Z=\min(Z_1,Z_2)$ can be expressed as:

$$f_z(z)=2f_{Z_i}(z)(1-F_{Z_i}(z)),\ i\in\{1,2\} \tag{14}$$

Substituting (11) and (12) into (**??**) yields the result in (13).

4. Application to the P_{FA}'s evaluation of CFAR processors

Given the decision rule in (2) and the clutter level estimates defined in (1), the P_{FA} can be expressed as:

$$P_{FA}(T)=E_Z[\Pr(X_0>TZ\mid H_0)] \tag{15}$$

Since $X_0\sim$ Lévy(δ,γ), $\Pr(X_0>TZ\mid H_0)$ can be written as:

$$\Pr(X_0>TZ\mid H_0)=1-F_{X_0}(TZ)=\operatorname{erf}\left(\sqrt{\frac{\gamma}{2(TZ-\delta)}}\right). \tag{16}$$

Substituting (15) into (16) gives:

$$P_{FA}(T)=\int_{-\infty}^{+\infty}\operatorname{erf}\left(\sqrt{\frac{\gamma}{2(TZ-\delta)}}\right)f_z(z)dz. \tag{17}$$

Now, substituting (5), (9), and (13) into (17) yields the P_{FA} expressions for the CA, GO, and SO-CFAR processors, given in (18), (19), and (20), respectively. Here, $T_{CA}=T/2N$, and $T_{GO}=T_{SO}=T/N$. The P_{FA} for the CA-CFAR processor is:

$$P_{FA,CA}(T_{CA})=\sqrt{\frac{2N^2\gamma}{\pi}}\int_{2N\delta}^{+\infty}\operatorname{erf}\left(\sqrt{\frac{\gamma}{2(T_{CA}z-\delta)}}\right)\frac{e^{-\frac{2N^2\gamma}{z-2N\delta}}}{(z-2N\delta)^{\frac{3}{2}}}dz. \tag{18}$$

$$P_{FA,GO}(T_{GO})=2\sqrt{\frac{N^2\gamma}{\pi}}\int_{N\delta}^{+\infty}\operatorname{erf}\left(\sqrt{\frac{\gamma}{2(T_{GO}z-\delta)}}\right)\operatorname{erfc}\left(\sqrt{\frac{N^2\gamma}{z-N\delta}}\right)\frac{e^{-\frac{N^2\gamma}{z-N\delta}}}{(z-N\delta)^{\frac{3}{2}}}dz. \tag{19}$$

$$P_{FA,SO}(T_{SO})=2\sqrt{\frac{N^2\gamma}{\pi}}\int_{N\delta}^{+\infty}\operatorname{erf}\left(\sqrt{\frac{\gamma}{2(T_{SO}z-\delta)}}\right)\operatorname{erf}\left(\sqrt{\frac{N^2\gamma}{z-N\delta}}\right)\frac{e^{-\frac{N^2\gamma}{z-N\delta}}}{(z-N\delta)^{\frac{3}{2}}}dz. \tag{20}$$

Remark 3 Although the integrals presented in (18), (19), (20), defy straightforward analytical evaluation since they cannot be expressed in a simple closed form, they are ready to be evaluated numerically. Thereby, we can unravel the underlying mathematical intricacies and extract meaningful results.

5. Numerical results

This section presents the numerical evaluation of the CA-, GO-, and SO-CFAR processors' performance under homogeneous non-centered Lévy-distributed clutter. Unless otherwise specified, for all simulations, we set $\gamma=1/\sqrt{2}$, and the size of the reference window is fixed at $N=8$. The results are derived using the analytical expressions in equations (18), (19), and (20) and validated through Monte Carlo simulations.

Figs. 1 (a), 1 (b), and 1 (c) illustrate the PFA performance as a function of the scaling factor T for the CA-, GO-,

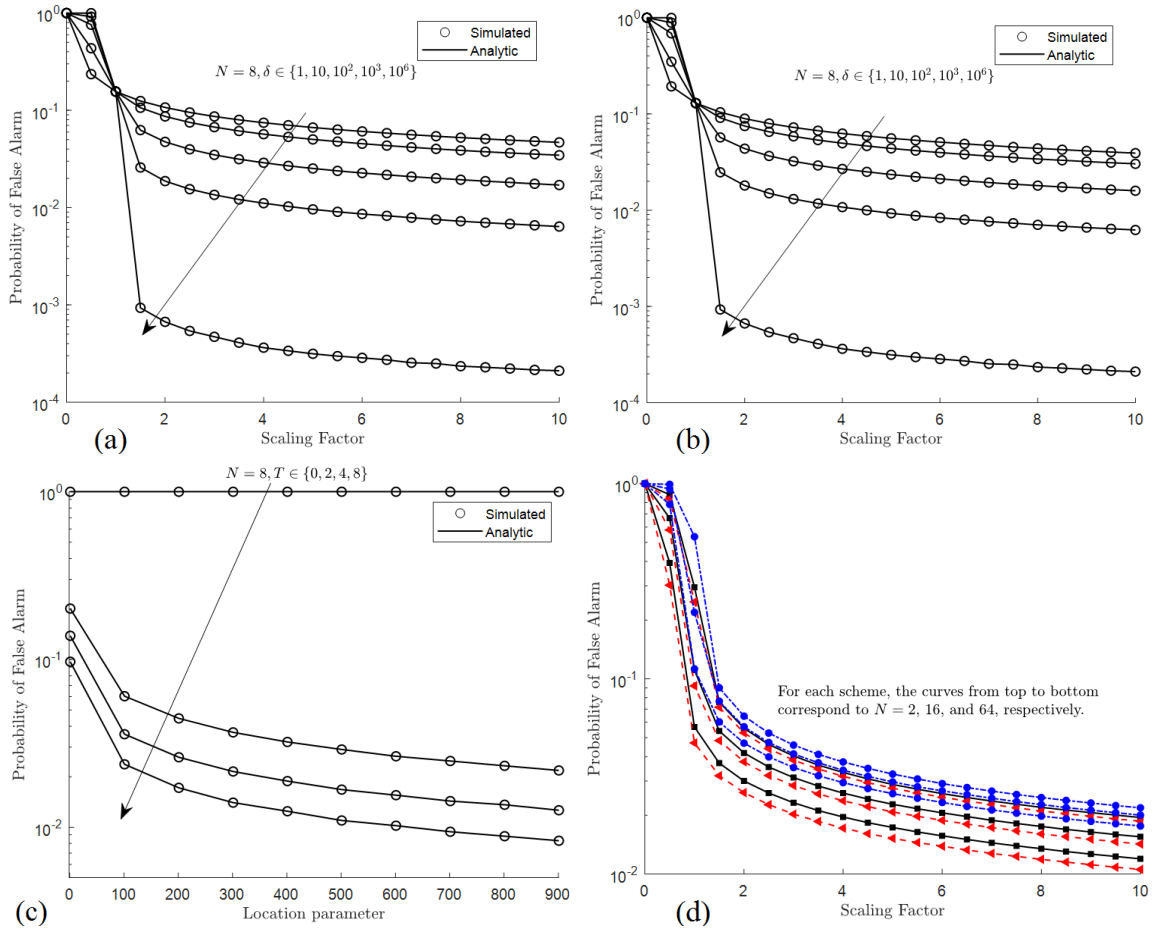

Figure 1. Probability of false alarm versus scaling factor of: (a) CA-CFAR, (b) GO-CFAR, (c) SO-CFAR, and (d) Comparison.

and SO-CFAR processors, respectively, across different values of the location parameter δ. The results indicate that P_{FA} declines decreases as T increases for all processors. Additionally, larger values of δ result in lower P_{FA}, demonstrating the influence of the clutter's location parameter on false alarm performance. For instance, in Fig. 1 (a), the CA-CFAR processor exhibits a steady decline in P_{FA} as T increases, with this trend becoming more pronounced for higher values of δ. Similar behavior is observed for GO- and SO-CFAR processors in Figs. 1 (b) and 1 (c), respectively.

Fig. 1 (d) compares the performance of all three processors for $\delta = 10^2$. The GO-CFAR processor demonstrates superior performance by maintaining consistently lower P_{FA} compared to CA-CFAR. However, the SO-CFAR processor shows significantly higher P_{FA} across all values of T, indicating its limited robustness in such scenarios. These results suggest that GO-CFAR is better suited for scenarios requiring stricter false alarm control, while SO-CFAR may not be ideal due to its elevated false alarm rates.

Figs. 2 (a), 2 (b), and 2 (c) depict how P_{FA} varies with δ for each processor at different values of T. Across all processors, increasing δ leads to a consistent reduction in P_{FA}, reflecting their adaptability to clutter environments with higher location parameters. For example, in Fig. 2 (a), the CA-CFAR processor exhibits a sharp decrease in P_{FA} as δ increases, particularly at lower values of T. Similar behavior is observed for GO- and SO-CFAR processors in Figs. 2 (b) and 2 (c), with differences in their sensitivity to changes in δ.

Fig. 2 (d) compares the three processors' performance as a function of δ for a fixed scaling factor $(T = 4)$. The GO-CFAR processor again outperforms CA-CFAR by achieving lower false alarm probabilities across all values of δ. In contrast, SO-CFAR's performance remains suboptimal due to its excessive reliance on smaller reference window sizes (N). For instance, when $N = 2$, SO-CFAR suffers from a significant performance degradation compared to CA- and GO-CFAR processors. This highlights its limited applicability in scenarios with small reference windows.

From these observations, we conclude that increasing either the scaling factor (T) or the location parameter (δ) reduces false alarm probabilities across all processors. The GO-CFAR processor consistently outperforms CA-CFAR in terms of P_{FA}, making it more suitable for stringent detection requirements. However, the SO-CFAR processor exhibits poor performance under small reference window sizes (N), limiting its applicability in certain scenarios. These findings provide valuable insights into how key parameters influence CFAR processor performance and guide their selection based on operational requirements and clutter characteristics.

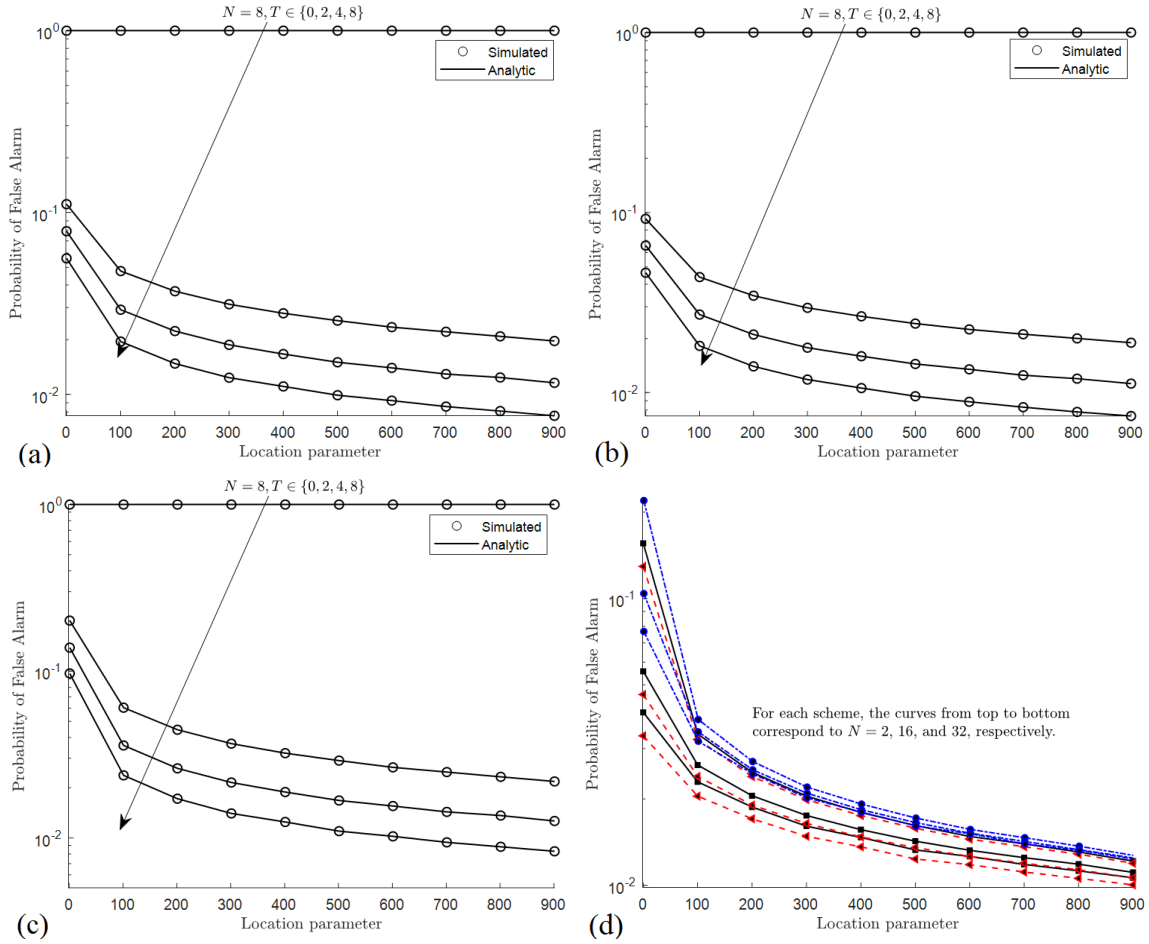

Figure 2. Probability of false alarm versus location parameter of : (a) CA-CFAR, (b) GO-CFAR, (c) SO-CFAR, and (d) Comparison.

6. Conclusion

In this work, we have carried out a performance analysis of CA-, GO-, and SO-CFAR processors in the case of a homogeneous non-centered Lévy-distributed clutter. To this end, we have derived the key statistical properties for the clutter's mean level in a form of the sum, maximum sum, and minimum sum of i.i.d non-centered Lévy RV' PDFs. On this basis, we have derived integral-form expressions for the aforementioned processors' P_{FA}s. These expressions provide a practical framework for the analysis and design of CFAR processors. Furthermore, we have examined various parameters and their impact on the performance of the studied processors. The numerical findings indicate that increasing the clutter's location parameter δ improves the processors' performances. Future research will focus on heterogeneous environments, adaptive CFAR techniques, and ML-based approaches for threshold optimization to provide a complete evaluation of CFAR detectors in non-Gaussian clutter. Furthermore, with a view to empirical validation, one of the main future efforts will be to incorporate real data in order to adapt the non-centered Lévy distribution to actual clutter returns.

Authors contributions
Authors have contributed equally in preparing and writing the manuscript.

Availability of data and materials
The data that support the findings of this study are available from the corresponding author upon reasonable request.

Conflict of interests
The authors declare that they have no known competing financial interests or personal relationships that could have appeared to influence the work reported in this paper.

References

[1] P. P. Gandhi and S. A. Kassam. "**Analysis of CFAR processors in nonhomogeneous background**.". *IEEE Trans. Aerosp. Electron. Syst.*, 24(4):427–445, 1988.
DOI: https://doi.org/10.1109/7.7185.

[2] Z. Dai, P. Wang, H. Wei, and Y. Xu. "**Adaptive detection with constant false alarm ratio in a non-Gaussian noise background**.". *IEEE Commun. Lett.*, 23(8):1369–1372, 2019.
DOI: https://doi.org/10.1109/lcomm.2019.2918816.

[3] J. Zhou and J. Xie. "**Performance analysis of linearly combined order statistics CFAR processors in heterogeneous background**.". *IEEE Trans. Aerosp. Electron. Syst.*, pages 1–10, 2023.
DOI: https://doi.org/10.1109/taes.2023.3339405.

[4] Z. Chen, A. Chen, W. Liu, , and X. Ma. "**CFAR detection in nonhomogeneous Weibull sea clutter for skywave OTHR**.". *IEEE*

Geosci. Remote Sens. Lett., 20:1–5, 2023.
DOI: https://doi.org/10.1109/lgrs.2023.3313179.

[5] P. P. Gandhi and S. A. Kassam. "**Optimality of the cell averaging CFAR detector**.". *IEEE Trans. Inf. Theory*, 40:1226–1228, 1994.
DOI: https://doi.org/10.1109/18.335950.

[6] V. G. Hansen and J. H. Sawyers. "**Detectability Loss due to Greatest-of Selection in a Cell Averaging CFAR**.". *IEEE Trans. Aerosp. Electron. Syst.*, AES-16:115–118, 1980.
DOI: https://doi.org/10.1109/taes.1980.308885.

[7] M. Weiss. "**Analysis of Some Modified Cell-Averaging CFAR Processors in Multiple-Target Situations**.". *IEEE Trans. Aerosp. Electron. Syst.*, AES-18(1):102–114, 1982.
DOI: https://doi.org/10.1109/taes.1982.309210.

[8] G. V. Trunk. "**Range resolution of targets using automatic detectors**.". *IEEE Trans. Aerosp. Electron. Syst.*, AES-14(5):750–755, 1978.
DOI: https://doi.org/10.1109/taes.1978.308625.

[9] J. T. Rickard and G. M. Dillard. "**Adaptive detection algorithm for multiple target situations**.". *IEEE Trans. Aerosp. Electron. Syst.*, AES-13(4):338–343, 1977.
DOI: https://doi.org/10.1109/taes.1977.308466.

[10] Y. Sim, J. Heo, Y. Jung, S. Lee, and Y. Jung. "**FPGA Implementation of Efficient CFAR Algorithm for Radar Systems**.". *Sensors*, 23(2):954, 2023.
DOI: https://doi.org/10.3390/s23020954.

[11] T. H. Kerbaa, A. Mezache, and H. Oudira. "**Improved Decentralized SO-CFAR and GO-CFAR Detectors via Moth Flame Algorithm**.". *International Conference of Advanced Technology in Electronic and Electrical Engineering (ICATEEE)*, pages 1–5, 2022.
DOI: https://doi.org/10.1109/icateee57445.2022.10093725.

[12] L. P. Jiménez Jiménez, F. D. A. García, M. C. L. Alvarado, G. Fraidenraich, and E. R. d. Lima. "**A General CA-CFAR Performance Analysis for Weibull-Distributed Clutter Environments**.". *IEEE Geosci. Remote Sens. Lett.*, 19:1–5, 2022.
DOI: https://doi.org/10.1109/lgrs.2022.3187554.

[13] M. C. Luna Alvarado, F. D. A. García, L. P. J. Jiménez, G. Fraidenraich, and Y. Iano. "**Performance evaluation of SOCA CFAR detectors in Weibull-distributed clutter environments**.". *IEEE Geosci. Remote Sens. Lett.*, 19:1–5, 2022.

[14] H. Rohling. "**Radar CFAR thresholding in clutter and multiple target situations**.". *IEEE Trans. Aerosp. Electron. Syst.*, AES-19: 608–621, 1983.
DOI: https://doi.org/10.1109/taes.1983.309350.

[15] M. Guida, M. J. Longo, and M. Lops. "**Biparametric CFAR procedures for lognormal clutter**.". *IEEE Trans. Aerosp. Electron. Syst.*, 29:798–809, 1993.
DOI: https://doi.org/10.1109/7.220931.

[16] R. Rifkin. "**Analysis of CFAR performance in Weibull clutter**.". *IEEE Trans. Aerosp. Electron. Syst.*, 30:315–329, 1994.
DOI: https://doi.org/10.1109/7.272257.

[17] S. Watts. "**Cell-averaging CFAR gain in spatially correlated k-distributed clutter**.". *IEEE Proc.-Radar Sonar Navig.*, 143(5): 321–327, 1996.
DOI: https://doi.org/10.1049/ip-rsn:19960745.

[18] G. V. Weinberg. "**Constant false alarm rate detectors for Pareto clutter models**.". *IET Radar Sonar Navig.*, 7(2):153–163, 2013.
DOI: https://doi.org/10.1049/iet-rsn.2011.0374.

[19] V. A. Aalo, K. P. Peppas, and G. Efthymoglou. "**Performance of CA-CFAR detectors in nonhomogeneous positive alpha stable clutter**.". *IEEE Trans. Aerosp. Electron. Syst.*, (3):2027–2038, 2015.
DOI: https://doi.org/10.1109/taes.2015.140043.

[20] M. Y. Rihan, Z. B. Nossair, and R. I. Mubarak. "**An improved CFAR algorithm for multiple environmental conditions**.". *Signal Image Video Process. (SIViP)*, 18:3383–3393, 2024.
DOI: https://doi.org/10.1007/s11760-024-03001-x.

[21] P. Tsakalides, F. Trinic, and C. L. Nikias. "**Performance assessment of CFAR processors in Pearson-distributed clutter**.". *IEEE Trans. Aerosp. Electron. Syst.*, 36(4):1377–1386, 2000.
DOI: https://doi.org/10.1109/7.892685.

[22] A. Meziani and F. Soltani. "**Performance Analysis of Some CFAR Detectors in Homogeneous and Non-Homogeneous Pearson-Distributed Clutter**.". *Signal Process.*, 86(8):2115–2122, 2006.
DOI: https://doi.org/10.1016/j.sigpro.2006.02.036.

[23] Y. Zhang, X. Wang, and S. Zhang. "**Persymmetric Adaptive Target Detection With Dual-Polarization in Compound Gaussian Sea Clutter With Inverse Gamma Texture**.". *IEEE J. Ocean. Eng.*, 47 (1):1–14, 2022.
DOI: https://doi.org/10.1109/tgrs.2022.3207809.

[24] X. Li, Y. Wang, and X. Zhang. "**Adaptive Persymmetric Subspace Detection in Non-Gaussian Sea Clutter With Structured Interference**.". *IEEE Geosci. Remote Sens. Lett.*, 19:1–5, 2022.
DOI: https://doi.org/10.1109/tgrs.2024.3374270.

[25] A. Salehi, M. Imani, A. Zaimbashi, and H. Yanikomeroglu. "**Learning and model-based approaches for radar target detection**.". *IEEE Trans. Cogn. Commun. Netw.*, 10(5):1817–1830, 2024.
DOI: https://doi.org/10.1109/tccn.2024.3391327.

[26] K. Zebiri and A. Mezache. "**CFAR detection using two scale invariant functions in heterogeneous Weibull clutter**.". *Signal Image Video Process. (SIViP)*, 18:7285–7291, 2024.
DOI: https://doi.org/10.1007/s11760-024-03393-w.

[27] M. C. Luna Alvarado, F. D. A. García, L. P. J. Jiménez, G. Fraidenraich, and Y. Iano. "**Performance evaluation of SOCA-CFAR detectors in Weibull-distributed clutter environments**.". *IEEE Geosci. Remote Sens. Lett.*, 19:1–5, 2022.
DOI: https://doi.org/10.1109/lgrs.2022.3152936.

[28] A. Abbadi, H. Bouhedjeur, A. Bellabas, T. Menni, and F. Soltani. "**Generalized closed-form expressions for CFAR detection in heterogeneous environment**.". *IEEE Geosci. Remote Sens. Lett.*, 15(7): 1011–1015, 2018.
DOI: https://doi.org/10.1109/lgrs.2018.2822782.

[29] I. Garvanov. "**Probability characteristics of CFAR processors in presence of randomly arriving impulse interference**.". *Proc. Int. Conf. Telecommun. Remote Sens., Cham*, page 17–32, 2023.
DOI: https://doi.org/10.1007/s11760-024-03480-y.

[30] M. Baadeche, M. A. Bouteldja, and F. Soltani. "**Target detection performance analysis for MIMO radars in gamma environment**.". *Signal Image Video Process.(SIViP)*, 18:8379–8385, 2024.
DOI: https://doi.org/10.1007/s11760-024-03480-y.

[31] W. Zhou, J. Xie, G. Li, and Y. Du. "**Robust CFAR detector with weighted amplitude iteration in nonhomogeneous sea clutter**.". *IEEE Trans. Aerosp. Electron. Syst.*, 53:1520–1535, 2017.
DOI: https://doi.org/10.1109/taes.2017.2671798.

[32] W. Zhou, J. Xie, B. Zhang, and G. Li. "**Maximum likelihood detector in Gamma-distributed sea clutter**.". *IEEE Geosci. Remote Sens. Lett.*, 15:1705–1709, 2018.
DOI: https://doi.org/10.1109/lgrs.2018.2859785.

[33] M. Sahed, E. Kenane, A. Khalfa, and F. Djahli. "**Exact closed-form PFA expressions for CA- and GO-CFAR detectors in gamma-distributed radar clutter**.". *IEEE Trans. Aerosp. Electron. Syst.*, 59: 4674–4679, 2023.
DOI: https://doi.org/10.1109/taes.2022.3232101.

[34] I. S. Gradshteyn, I. M. Ryzhik, D. Zwillinger, and V. Moll. "**Table of Integrals, Series, and Products**.". *8th ed. Amsterdam: Academic Press*, 2014.
DOI: https://doi.org/10.1016/C2010-0-64839-5.